Infrared pulsed fiber lasers employing 2D nanomaterials as saturable absorbers

Yong Liu*, Heping Li, Jianfeng Li
State Key Laboratory of Electronic Thin Films and Integrated Devices, School of Optoelectronic Information, University of Electronic Science and Technology of China (UESTC), Chengdu 610054, China

ABSTRACT

We demonstrate that two kinds of 2D nanomaterials are employed as saturable absorbers to realize infrared pulsed fiber lasers at 1.5 μm and 3 μm, respectively. Mode-locked optical pulses are achieved at 1.5 μm erbium-doped fiber lasers by using multilayer molybdenum disulfide (MoS_2). In addition, Q-switched fiber lasers are realized at 3 μm region by using topological insulator:Bi_2Te_3. Experimental proofs are provided. Our work reveals that 2D nanomaterials like MoS_2 and TI: Bi_2Te_3 are absolutely a class of promising and reliable saturable absorbers for optical pulse generation at infrared waveband.

Keywords: pulsed fiber laser, 2D nanomaterials, Q-switching, mode locking

1. INTRODUCTION

Pulsed fiber lasers have attracted considerable interest due to their various practical applications in optical communication, frequency metrology, military systems and laser micromachining. Compared to actively pulsed fiber laser, passive ones are more compact and flexible thus favored in some practical applications.

Various material saturable absorbers have been applied in the passively pulsed schemes, e.g., semiconductor saturable absorber mirror (SESAM), Fe^{2+}:ZnSe crystal, and some nanomaterials like single wall carbon nanotubes (SWCNTs) and graphene. In particular, graphene behaves as an excellent saturable absorber for achieving broadband absorption spectral range due to the unique zero band gap and ultrafast saturable absorption properties [1]. The success of graphene greatly motivates the exploration of other graphene-like two dimensional (2D) materials for practical applications. Recently, molybdenum disulfide (MoS_2) and topological insulators (TIs) arose and drew focused attention due to their special characteristics. For example, TI has a significantly higher modulation depth of typically as high as 98% (normalized), and higher damage threshold, which are beneficial to achieve narrow and energetic Q-switched pulses.

In this paper, we report pulsed fiber lasers using MoS_2 and TIs as saturable absorbers. We present an erbium-doped fiber laser mode-locked by a MoS_2-based saturable absorber [2]. The chemical vapor deposition (CVD) method is employed to grow high-quality multilayer MoS_2, which is subsequently transferred onto the end-face of a fiber connector in the fiber laser. Stable mode-locked soliton pulses are achieved at a pump threshold of 31 mW, the output pulses have central wavelength, spectral width, pulse duration, and repetition rate of 1568.9 nm, 2.6 nm, 1.28 ps, and 8.288 MHz, respectively. We also report a high energy passively Q-switched Ho^{3+}-doped ZBLAN fiber laser at 2979.9 nm using TI: Bi_2Te_3 as saturable absorber [3]. TI: Bi_2Te_3 nanosheets are synthesized using the cost-effective hydrothermal intercalation/exfoliation method. The ethanol solution dispersing the TI: Bi_2Te_3 nanosheets are dropped on a CaF_2 substrate to fabricate the free-space saturable absorber component. Stable Q-switched pulses at 2979.9 nm are obtained with the repetition rate of 81.96 kHz and pulse duration of 1.37 μs. The achieved maximum output power and pulse energy are 327.4 mW at a slope efficiency of 11.6 % and 3.99 μJ respectively, only limited by the available pump power. Experimental results show that 2D nanomaterials are promising to act as saturable absorbers for realizing passive pulsed lasers at infrared waveband.

*YongLiu@uestc.edu.cn; phone 86 28 83206481; fax 86 28 83208199

Semiconductor Lasers and Applications VII, edited by Ninghua Zhu, Werner H. Hofmann,
Proc. of SPIE Vol. 10017, 100170P · © 2016 SPIE · CCC code: 0277-786X/16/$18
doi: 10.1117/12.2247594

2. MODE-LOCKED FIBER LASER USING MOS_2-BASED SATURABLE ABSORBER

2.1 Preparation of MoS_2-based saturable absorber

MoS_2 thin films were synthesized in a tube furnace by the CVD method [4]. In a typical growth, 500 mg of MoO_3 powder was placed in the center of the furnace and 500 mg of sulfur powder was placed at the upstream. Several pieces of Si wafer with 300 nm SiO_2 were used as substrates and placed downstream. The quartz tube was evacuated to a base pressure of 0.1 Torr, and then flowed with Ar gas, which was controlled by a mass flow controller. After the pressure stabilized, the furnace was heated to 550 ^oC at a rate of 25 ^oC /min and maintained for 30 min. The sulfur powder was heated by a twisted heating belt with the temperature of 100 ^oC. After the deposition, the furnace was naturally cooled to room temperature.

Surface morphology and height profile of the MoS_2 thin films were obtained using CSPM 5500 atomic force microscopy (AFM). Raman spectra were measured by Renishaw 100 Raman spectrometer with 514 nm laser. Figure 1a shows the optical microscopy image of multilayer MoS_2 film. One can find that the thin film is continuous and uniform over a large area. The Raman spectrum of the multilayer MoS_2 is shown in Figure 1b. The sample exhibits two characteristic peaks, in parallel with two phonon modes: out of plane vibration of S atoms at 406 cm^{-1}, and in plane vibration of Mo and S atoms at 381 cm^{-1}, with a frequency difference of 25 cm^{-1}. The frequency difference of the two modes can be used to determine the layer thickness of MoS_2. In our result, 25 cm^{-1} corresponds to 4-5 layers of MoS_2. A typical AFM image is shown in Figure 1c. The thickness of the film which can be determined by the height profile in Figure 1d is about 3.42 nm, corresponding to 5 layers of MoS_2.

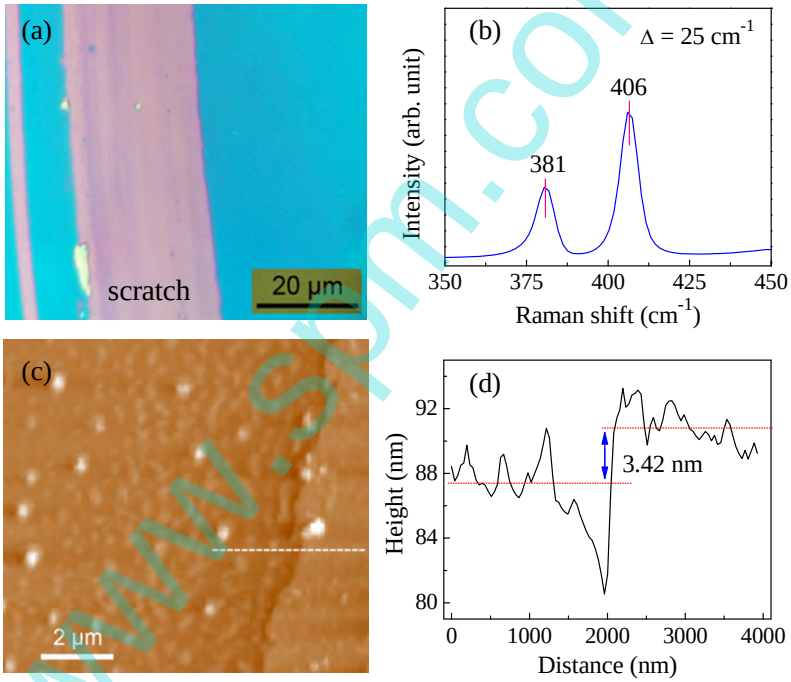

Figure 1. (a) Optical microscopy image of a typical multilayer MoS_2 film on SiO_2 substrate. Scratch was intentionally introduced to show the color contrast between the thin film and the substrate (no MoS_2 exists in the scratched region.). (b) Corresponding Raman spectrum, (c) AFM image, and (d) AFM height profile of across the dash line in (c).

For the transfer of multilayer MoS_2 film, PMMA was spin coated on the MoS_2 film. After 10 min baking at 100 ^oC, samples were immersed in hydrofluoric acid (30%) for a few seconds in order to lift off the PMMA-MoS_2 films. The PMMA-MoS_2 films were transferred to a deionized water to dilute and remove the etchant and residues. Then, the PMMA-MoS_2 film was transferred to end-face of a FC, followed by drying in air for 1 h. The PMMA was removed by acetone, isopropyl alcohol and then deionized water. The MoS_2 coated FC was connected to a clean FC with a fiber adapter to form the MoS_2-based mode locker.

2.2 Experimental setup and results

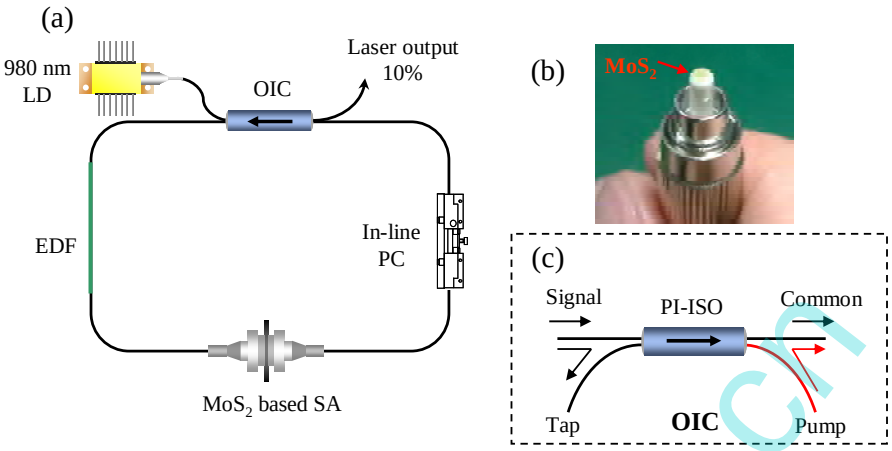

Figure 2. (a) A schematic diagram of the fiber ring laser. 980 nm LD: 980 nm diode laser pump source, OIC: optical integrated component, EDF: erbium-doped fiber, PC: polarization controller, MoS_2-based SA: MoS_2-based saturable absorber. (b) Photograph of a FC coated with multilayer MoS_2. (c) The schematic structure of the OIC. PI-ISO: polarization-insensitive isolator

The experimental setup of the mode-locked fiber ring laser is schematically shown in Figure 2a [2]. The cavity comprises of 0.8-m-long erbium doped fiber with group velocity dispersion (GVD) of 16 ps/(nm•km), a segment of 1.0-m HI 1060 Flex fiber with GVD of 8 ps/(nm•km), and a piece of 23.0-m standard single mode fiber. The chemical vapor deposition (CVD) method is employed to grow high-quality MoS_2, and the MoS_2 film is sandwiched between two fiber connectors with a fiber adapter, shown in Figure 2b. An optical integrated component (OIC) was used in the cavity, which has the combination functions of a wavelength-division multiplexer, an output coupler, and a polarization-insensitive isolator (PI-ISO). The structure of the OIC is schematically shown in Figure 2c. The pump light is launched into the OIC through the port of the pump and then reflected into the common port by the pump-reflective coating. The signal laser propagates into the OIC from the input port and partly reflected into the tap port by the 10% signal-reflective coating. The center part of the OIC is a PI-ISO which ensures the unidirectional operation.

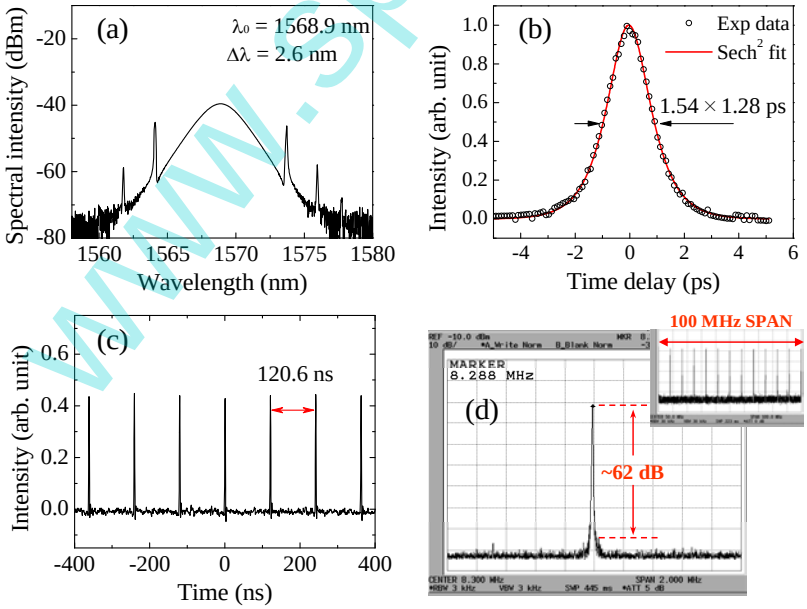

Figure 3. Mode-locking performance of the fiber laser mode-locked by a multilayer MoS_2-based saturable absorber. (a) Optical spectrum. (b) Autocorrelation trace. (c) Pulse train. (d) RF spectrum with a 2 MHz span and 3 kHz resolution bandwidth. Inset: RF spectrum in 100 MHz span.

When the pump power was increased to 31 mW, the self-starting mode locking was achieved. Figure 3a shows the optical spectrum of mode locked pulses. The spectrum is centered at 1568.9 nm and the 3-dB spectral width is 2.6 nm. Several pairs of sidebands are symmetrically distributed at both sides of the spectrum, which is the typical characteristic of conventional soliton pulses. A measured autocorrelation trace is shown in Figure 3b. It has a full width at half maximum (FWHM) width of 1.97 ps. Figure 3c shows the oscilloscope trace of the mode-locked pulse train. The time interval between the pulses is ~120.6 ns. Figure 3d presents the corresponding RF spectrum with a 2 MHz span and 3 kHz resolution bandwidth. The repetition rate of the soliton pulses is 8.288 MHz, matching exactly with the cavity roundtrip time of ~120.6 ns and the cavity length of ~24.8 m. The signal-to-noise ratio (SNR) is ~62 dB, indicating good mode-locking stability. The RF spectrum with a 100 MHz span shown in the inset of Figure 3d illustrates stable operation of the pulsed laser without exhibiting a Q-switching instability. The fundamental mode locking operation was maintained up to a pump power of ~152 mW. The maximum output power was 5.1 mW and the corresponding pulse energy was estimated to be 0.615 nJ.

3. Q-SWITCHED HO^{3+}-DOPED ZBLAN FIBER LASER USING TI-BASED SATURABLE ABSORBER

3.1 Preparation of TI: Bi_2Te_3 nanosheets

TI: Bi_2Te_3 nanosheets were synthesized using the cost-effective hydrothermal intercalation/exfoliation method [5]. The ethanol solution dispersing the TI: Bi_2Te_3 nanosheets were dropped on a CaF_2 substrate to fabricate the free-space saturable absorber component. Then a series of characterizations were performed to reveal the performance of our saturable absorber. Figure 4a and 4b show the measured SEM images of our TI: Bi_2Te_3 sample by field-emission scanning electron microscopy. The lower magnification SEM image as shown in Figure 4a reveals many predominantly hexagonal-based sheets with uniform size and well-defined shape are randomly dispersed. The higher magnification SEM image as shown in Figure 4b shows that the edge length of the sheets is at the range of 300~400 nm. Figure 4c is the measured Raman spectrum of our TI: Bi_2Te_3 sample. Three typical optical phonon peaks identified as A^1_{1g}, A^2_g, and A^2_{1g} are located at 64.81 cm^{-1}, 103.43 cm^{-1}, 140.90 cm^{-1}, respectively. Besides, an additional peak A^2_{1u} with strongest intensity locating at 121.20 cm^{-1} is also observed resulting from the symmetry breaking in atomically thin films. It indicates that the prepared TI: Bi_2Te_3 sample was in a great nano-structured state. Figure 4d shows the measured AFM image and its corresponding height profile of the TI: Bi_2Te_3 sample. The results suggest its average thickness is at the range of 7.11~10.37 nm.

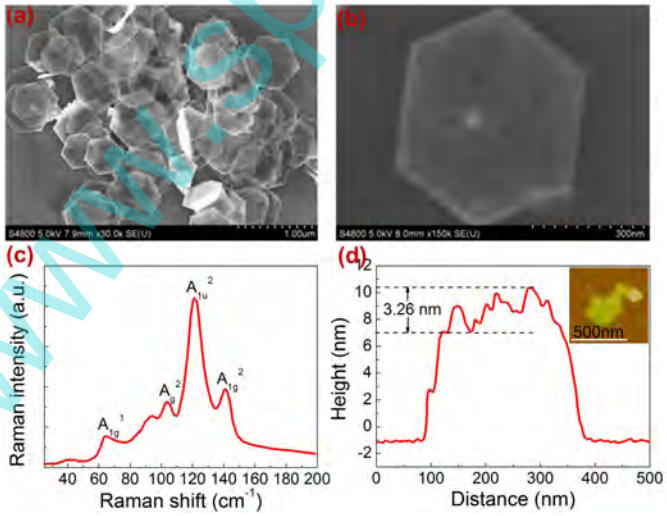

Figure 4. (a) Lower and (b) higher magnification SEM images, (c) Raman spectrum, and (d) AFM image (inset) and its corresponding height profile of the TI: Bi_2Te_3 sample.

3.2 Experimental setup and results

The experimental setup of our constructed passively Q-switched Ho^{3+}-doped ZBLAN fiber laser is shown in Figure 5 [3]. Two commercially available high power 1150 nm diode lasers were employed to pump the gain fiber after polarization multiplexing via a polarized beam splitter (PBS) and focusing by a 1150 nm AR-coated ZnSe objective lens

with a 6.0 mm focal length acting as the collimator for the light out-coupled from the fiber core as well. The gain fiber is a piece of commercial double-cladding Ho^{3+}-doped ZBLAN fiber having a circular-shaped pump core with a diameter of 123 μm and NA of 0.5. The dopant concentration was 2.0 mol.%, thus the selected 5.2 m fiber can provide 92% pump absorption efficiency. A confocal arrangement consisting of two same plano-covex CaF_2 lens is inserted between the above ZnSe objective lens and protected gold mirror along the light path. The fabricated TI: Bi_2Te_3 saturable absorber component is firstly fixed in a mount connected with an one-dimension mobile platform along the light path and then placed in the confocal arrangement with an optimized position.

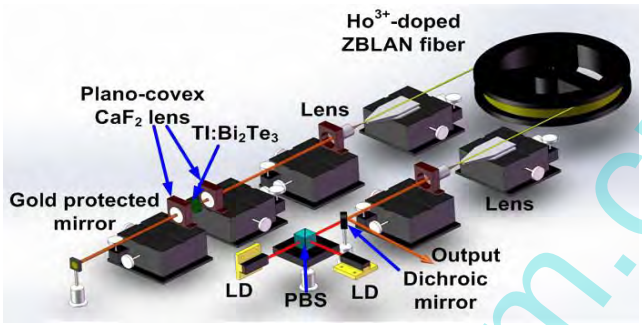

Figure 5. Experimental setup of the passively Q-switched Ho^{3+}-doped ZBLAN fiber laser based on the TI: Bi_2Te_3 saturable absorber.

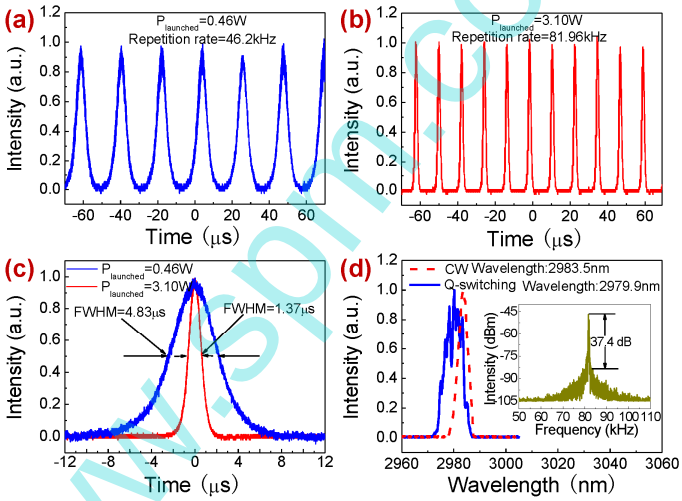

Figure 6. Q-switched pulse train at the launched pump power of (a) 0.46 W and (b) 3.10 W, (c) Q-switched single pulse waveform at the launched pump power of 0.46 W and 3.10 W, (d) optical spectra of CW laser and Q-switched pulses and RF spectrum (inset) of the Q-switched pulses at the launched pump power of 3.10 W.

The CW laser was firstly produced when the launched pump power was increased to 270 mW. Once it reached 464 mW, stable Q-switching was observed with a pulse duration of 4.83 μs and a repetition rate of 46.20 kHz, as shown in Figure 6a and 6c. The stable Q-switching regime can be maintained until the maximum available launched pump power of 3.10 W, as shown in Figure 6b and 6c. The pulse duration and repetition rate were measured to be 1.37 μs and 81.96 kHz, respectively. The pulse amplitude fluctuation was calculated to be about ±3% indicating its high stability. The optical spectrum of the Q-switched pulses at the maximum pump power was measured and normalized, as shown in Figure 6d. The average wavelength of 2979.9 nm with a FWHM of 7.2 nm was obtained. The inset of Figure 6d is the measured RF spectrum of the Q-switched pulses at a scanning span of 60 kHz and a resolution bandwidth of 100 Hz. The SNR of 37.4 dB indicates the stable Q-switching. At this moment, whether removing the TI: Bi_2Te_3 saturable absorber away from the cavity or moving the focused beam spot onto the clean region of the TI: Bi_2Te_3 partly covered CaF_2 substrate, the laser immediately recovered to the CW emission state identified by the oscilloscope due to lack of modulation factor. Note that the laser temporal performance in both cases were also monitored during the whole available pump range, the

unchanged CW emission state excluded the possibility of self-pulsing. The corresponding optical spectrum at the launched pump power of 3.10 W was also measured and shown in Figure 6d as a comparison.

4. CONCLUSIONS

We demonstrate that both MoS_2 and TI: Bi_2Te_3 function well as saturable absorbers to realizing passive pulsed fiber lasers at infrared waveband. We realize ultrashort pulse generation in an erbium-doped fiber laser mode-locked by using multilayer MoS_2-based saturable absorber, the compact all-fiber laser emitted stable mode-locked soliton pulses centered at 1568.9 nm with spectral width of 2.6 nm and pulse duration of 1.28 ps. In addition, a passively Q-switched Ho^{3+}-doped ZBLAN fiber laser at 2979.9 nm employing TI: Bi_2Te_3 is demonstrated. At the available maximum pump power of 3.10 W, maximum repetition rate of 81.96 kHz and shortest pulse duration of 1.37 μs is obtained. Our results suggest that 2D nanomaterials like MoS_2 and TI: Bi_2Te_3 are absolutely a class of high-performance broadband saturable absorbers at infrared waveband.

ACKNOWLEDGEMENT

This work was supported by National Nature Science Foundation of China (Grant No. 61435003, 61327004, 61435010, 61421002)

REFERENCES

[1] Bonaccorso, F., Sun, Z., Hasan, T. and Ferrari, A., "Graphene photonics and optoelectronics, " Nature Photonics 4(9), 611-622 (2010).

[2] Handing Xia, Heping Li, Changyong Lan, Chun Li, Xiaoxia Zhang, Shangjian Zhang and Yong Liu, "Ultrafast erbium-doped fiber laser mode-locked by a CVD-grown molybdenum disulfide (MoS_2) saturable absorber, " Optics Express 14(22), 17341-17348 (2014).

[3] Jianfeng Li, Hongyu Luo, Lele Wang, Chujun Zhao, Han Zhang, Heping Li and Yong Liu, "3μm mid-infrared pulse generation using topological insulator as the saturable absorber," Optics Letters, 15(40), 3659-3662 (2015).

[4] Najmaei, S., Liu, Z., Zhou, W., Zou, X., Shi, G., Lei, S., Yakobson, B. I., Idrobo, J.-C., Ajayan, P. M., and Lou, J., "Vapour phase growth and grain boundary structure of molybdenum disulphide atomic layers," Nature Mater. 12(8), 754-759 (2013).

[5] Ren, L., Qi, X., Liu, Y. D., Hao, G. L., Huang, Z. Y., Zou, X. H., Yang, L. W., Li, J., and Zhong, J. X., "Large-scale production of ultrathin topological insulator bismuth telluride nanosheets by a hydrothermal intercalation and exfoliation route, " J. Mater. Chem. 22, 4921-4926 (2012).